Underlying Control Strategy of Human Leg Posture and Movement

Shinsuk Park*
Department of Mechanical Engineering, Keio University,
3-14-1 Hiyoshi, Kohoku-ku, Yokohama, Japan 223-8522

While a great number of studies on human motor control have provided a wide variety of viewpoints concerning the strategy of the central nervous system (CNS) in controlling limb movement, none were able to reveal the exact methods how the movement command from CNS is mapped onto the neuromuscular activity. As a preliminary study of human-machine interface design, the characteristics of human leg motion and its underlying motor control scheme are studied through experiments and simulations in this paper. The findings in this study suggest a simple open-loop motor control scheme in leg motion. As a possible candidate, an equilibrium point control model appears consistent in recreating the experimental data in numerical simulations. Based on the general leg motion analysis, the braking motion by the driver's leg is modeled.

Key Words : Human Motor Control, Equilibrium Point Control Hypothesis, Braking Motion

1. Introduction

Studies on human motor control have provided a wide variety of viewpoints concerning the strategy of the central nervous system (CNS) in controlling limb movement. Among them several researchers have suggested the control of mechanical impedance as an important means of human motor control, where stiffness, damping and mass are the three basic components of mechanical impedance. Theoretical and experimental investigations of multi-jointed limbs have shown that the co-activation of agonist-antagonist muscle pairs at a joint controls its equilibrium angle and its stiffness, or more generally its impedance, independently.

Several studies on arm movement proposed that the stiffness characteristic of the arm endpoint is "spring-like" for small displacement about an equilibrium point (Mussa-Ivaldi et al., 1985). They characterized the stiffness of human arm using ellipse representing the restoring force field about the equilibrium point. In her study on human arm reaching motion, Flash (1987) suggested the CNS temporally shifts the desired equilibrium position and the viscoelastic property of muscles allows the arm to follow the desired trajectory.

The full characterization of human limb characteristics is applicable to the design of a variety of human-machine interfaces, such as pedal, joystick, and steering wheel. In designing brake pedal, for example, the characteristics of human leg motion should be taken into account. While braking appears to be a simple action, many drivers still have problems in managing the brake pedal. Little is known about the mechanisms of musculo-skeletal motor control in the driver's braking motion ; few studies have investigated this operation.

The purpose of this study is to investigate the characteristics of human leg motion and its underlying motor control through experiments and

* **E-mail** : sspark@alum.mit.edu
TEL : +81-45-563-1151; **FAX** : +81-45-566-1516
Department of Mechanical Engineering, Keio University, 3-14-1 Hiyoshi, Kohoku-ku, Yokohama, Japan 223-8522. (Manuscript **Received** October 6, 2003; **Revised** January 30, 2004)

simulations. The characteristics of human leg, leg endpoint stiffness and its movement, are analyzed in the framework of equilibrium point control (EPC) theory.

In section 2, experiments to measure human leg stiffness and motions are present, as well as brief background on pertinent human motor control. From the experimental results a simple model for testing the motor control of foot reaching motion is developed. Simulation results using this model are compared with experimental results. Section 3 discusses the results and summarizes the work. In section 4, the results from this study are provided.

2. Human Leg Motion Anlysis

This section introduces brief background on human movement generation and examines the characteristics of human leg motion and the underlying motor control scheme through experiments and simulations. Characteristics of the human leg were explored through measurements of simple reaching motion, impulsive motion, and postural stiffness. Computer simulations of a mathematical model of the human leg are carried out to recreate the experimental result of a simple reaching motion.

2.1 On human movement generation

There have been a great number of studies that attempted to reveal the basic properties of the human motor control system, but none were able to explain the exact methods of mapping the desired movement intention into the neuromuscular activity. It seems, however, natural to assume that there exists a hierarchy that underlies the human motor behavior. In human motor control, a multi-staged process that transforms sensory input into motor output seems consistent with known neural architectures (Berstein, 1967; Arbib, 1972). Indeed, it is an implicit assumption in most of human motor control studies.

Under the assumption, the production of motor behavior occurs in at least two stages: planning and execution. Many limb movements appear to be planned at a kinematic level. Morasso (1981) suggested that the central command for hand reaching motion is formulated in body-centered Cartesian coordinates. Even if movements are planned according to the kinematics of limb motion, the dynamics of the musculo-skeletal system have heavy influences in executing that plan. Inertial dynamics involves the Coriolis and centrifugal forces between body segments, which introduces nonlinearity.

Many studies have attempted to explain how human motor control system circumvents the complexity of multi-link dynamics. One of them is the "inverse dynamics" approach. Hollerbach and Atkerson (1987) proposed that the CNS solves the inverse dynamics problem to derive the necessary muscle forces from the desired trajectory. It implies that the CNS explicitly carries out extremely demanding computations. An alternative approach proposes a "look-up table" instead of the complex inverse dynamics computations (Albus, 1975; Raibert, 1976). This approach seems less likely due to the large size of the table. A much simpler approach suggests that the CNS utilizes effective mechanical property of the muscles and neural feedback circuits to circumvent the computational complexities of multi-joint motions. The neuromuscular system has the "spring-like" property: the muscle force varies with muscle length under controlled neural input. The co-contraction action of a group of muscles, agonists and antagonists, about a single joint allows the joint's equilibrium angle and its impedance to be adjusted independently. This suggests that CNS generates a series of equilibrium points for a limb, and the "spring-like" properties of the neuromuscular system drive the limb to follow the trajectory of the intermediate equilibrium points. This equilibrium point hypothesis may apply to the control of both static posture and dynamic movement (Bizzi et al., 1992).

Figure 1 illustrates a mechanism of the equilibrium point control in one-dimensional motion. In the figure mass M is driven by the force caused by stiffness K, damping B, and the difference between equilibrium position x_o and actual position x. Here, equilibrium position x_o serves

as a control input to the simple mechanical system. Flash (1987) demonstrated that the equilibrium point control can be used to model two-link planar reaching motions of the arm at moderate speeds. Using experimentally measured stiffness and the equilibrium point trajectories with a bell-shaped velocity profile, the simulations captured the kinematic features of experimentally measured trajectories.

In limb movements, the actual trajectory depends on external perturbations as well as the equilibrium point trajectory, commanded impedance, and limb dynamics. Equilibrium point control applies the same strategy to tasks requiring interaction with the environment, unrestrained motions and the transition between the two. Control of contact force can also be achieved through the use of an equilibrium point. Simply moving the equilibrium point to a point within a contact object will cause the limb to exert a force on that object.

However, there have been years of controversy over the validity of the equilibrium point control hypothesis. Many investigators argued against the equilibrium point control hypothesis, claiming that the brain sends as a motor command only an equilibrium-point trajectory similar to the actual trajectory. They provided experimental evidence that the brain controls the movement, doing all the calculations to figure out all muscle activities. It is reasoned that complex computations are required to generate the motor command because of nonlinear interaction forces between many degrees of freedom of the limb (Pennisi, 1996; Gomi and Kawato, 1996). Indeed, there is considerable evidence that the motor control system takes into account the dynamic properties of the limb as can be seen in preprogrammed or anticipatory reactions (Shadmehr and Mussa-Ivaldi, 1994).

2.2 Experiments on human leg

Figure 2 shows a computer-controlled two-link manipulator and a human subject. The two-link manipulator measured the position of the foot and the force exerted by it. To eliminate the effect of gravity, subjects lay laterally so that their sagittal planes were parallel to the horizontal plane, and the movements of their legs were contained in the plane. The trunk of the subject was fixed to the table, serving as a base. The hip and knee joints were free to move allowing a two degree-of-freedom motion. A brace was used to lock the ankle joint at 90°.

2.2.1 Reaching motion

In this experiment, subjects were instructed to move their feet between two unspecified targets as they would normally reach their feet from one point to another. Figure 3 shows the trajectories of foot reaching motion from four subjects. The trajectories were roughly straight. They show the same curvature, as if the center of curvature is placed in front of the subjects, while they all have different starting and finishing points. Figure 4

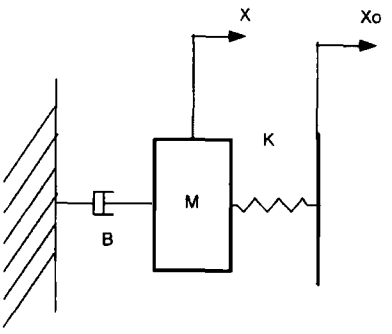

Fig. 1 One-dimensional model of equilibrium point control

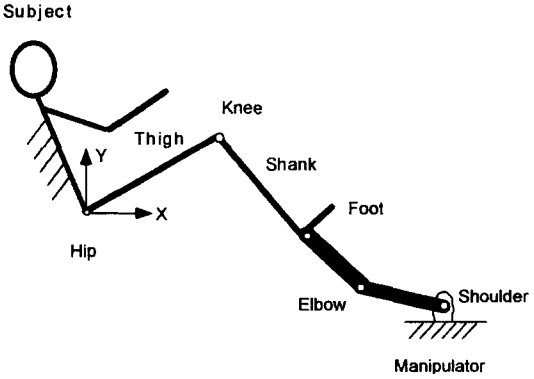

Fig. 2 Experimental setup for leg movement measurement

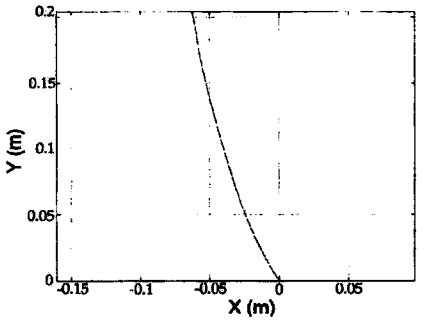

(a) Subject A

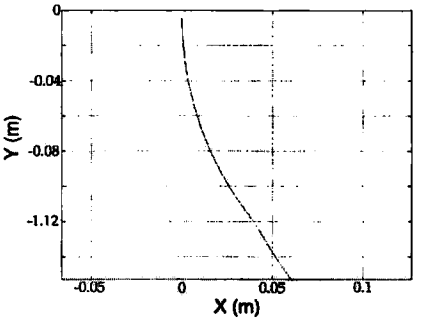

(b) Subject B

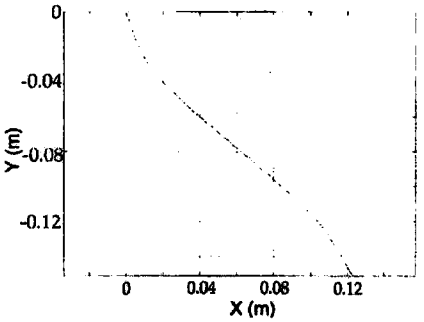

(c) Subject C

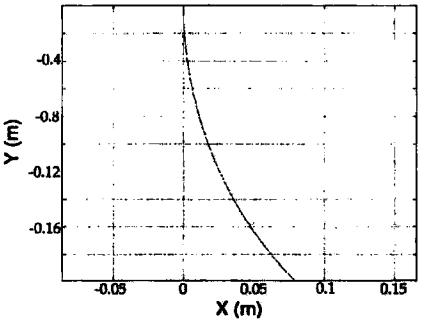

(d) Subject D

Fig. 3 Trajectories during foot reaching motion (Same coordinates as in Figure 2)

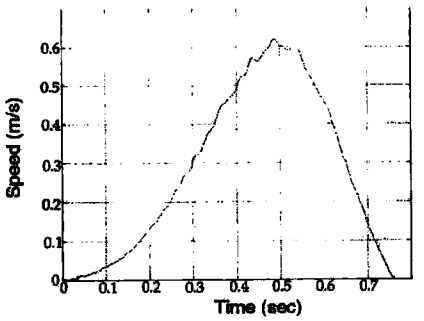

(a) Subject A

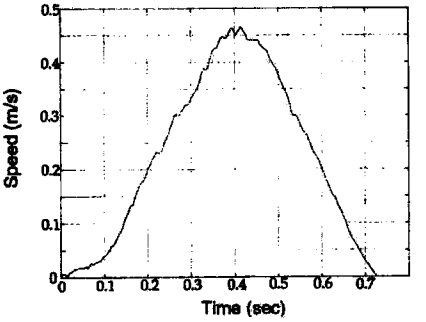

(b) Subject B

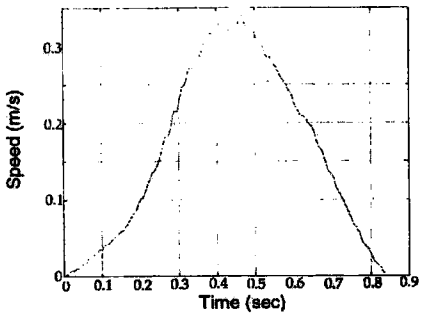

(c) Subject C

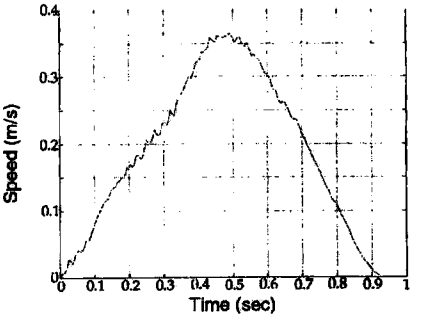

(d) Subject D

Fig. 4 Velocity profiles during foot reaching motion

shows velocities corresponding to the point-to-point movements. It is noteworthy that the velocity profiles have asymmetric unimodal bell shape.

2.2.2 Impulsive motion

In impulsive movement experiment, subjects were instructed to make a series of sharp jerky motions or kick-and-return motions of the foot. They were informed that the amplitude of their movements was not important but that they should attempt to make their movements as abrupt as possible. It was reasoned that an impulse as an extremely abrupt movement would include the highest frequency components that the subject was capable of producing. Thus, power spectral density was used as an estimation of the bandwidth of foot motion. Figure 5(a) illustrates the foot displacement from one subject during impulsive motion. Rise times were typically between 200 and 300 milliseconds. Figure 5(b) shows power spectral density of the displacement, where the unit of power spectral density is arbitrary. The bandwidth of the motion was lower than 5 Hz. It was reported that rise time for a human arm motion is around 60 milliseconds and that its bandwidth is between 20 and 30 Hz (Paines, 1987). The results in this study showed much slower leg response. This probably results from the fact that the human leg has larger inertia and longer limb length than the arm.

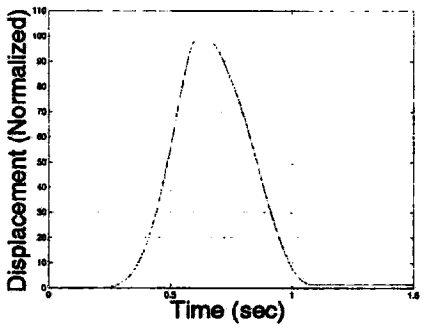

(a) Displacement during impulsive motion

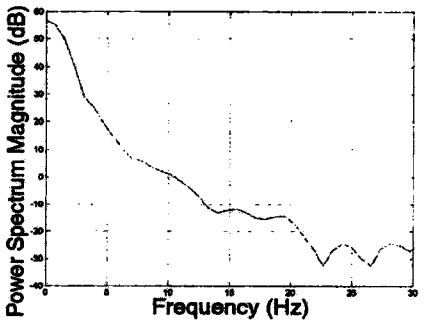

(b) Power spectral density of impulsive moton

Fig. 5 Impulsive motion (Subject *D*)

2.2.3 Postural stiffness

The static components of the human leg impedance were measured by a procedure similar to the experiment used by Mussa-Ivaldi et al.(1985) in their arm study. While no such tests had previously been performed for the lower limb, it seems reasonable to assume that common mechanisms apply to both the arm and the leg. The basic method is as follows: provide a perturbation that induces a displacement of the foot and then relate the evoked force to the input displacement to estimate the stiffness. The ankle of the subject was locked by a brace so that only the hip and knee joints were free. After the foot of the subject was moved to a reference position, displacements in three different directions were applied to the foot by a computer-controlled manipulator. The displacements were given in directions of 90°, 135° and 180° from the x-axis as shown in Figure 6. The magnitude of these displacements ranged from 3 to 5 cm, and the resulting displacement and force imposed at the foot were recorded. During the procedure, the subject was instructed "not to resist voluntarily,"

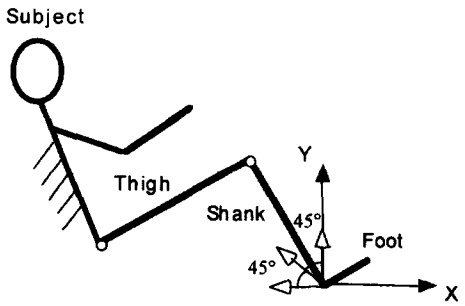

Fig. 6 Directions of displacement application in stiffness measurement

so that only passive static response would be measured.

From the data set collected in three directions, the stiffness field at the foot was estimated by the procedure similar to the experiment used by Mussa-Ivaldi et al.(1985). While the force-displacement function for muscle is fundamentally nonlinear, the function can be considered linear for small displacements about the equilibrium point. Therefore the two dimensional relationship of the displacement and corresponding force can be expressed as

$$\mathbf{F}=-\mathbf{K}\Delta\mathbf{x}$$

$$\begin{bmatrix}F_x\\F_y\end{bmatrix}=-\begin{bmatrix}K_{xx} & K_{xy}\\K_{yx} & K_{yy}\end{bmatrix}\begin{bmatrix}\Delta x\\\Delta y\end{bmatrix}$$

where F_x and F_y are the components of the restoring force, Δx and Δy are the components of the imposed displacement, and the elements of stiffness matrix K, K_{xx}, K_{xy}, K_{yx} and K_{yy}, are the linear stiffness terms in the posture. From three sets of force and displacement data measured in three directions, four elements of the linear stiffness matrix can be estimated.

The endpoint stiffness matrix estimation from force and displacement measurements are given in Table 1. The stiffness matrices are averaged from four experiments for each subject. The stiffness matrices can be characterized by their eigensolutions. The eigenvalues represent major and minor stiffness, and their corresponding eigenvectors represent their directions. Note that the minor stiffness is nearly null for subject D. Null stiffness implies that the leg can not impede the force applied in this direction.

The endpoint stiffness field measured at a reference posture can be transformed into the stiffness in joint space using the leg Jacobian matrix J_L. The joint stiffness K_J can be estimated as follows:

$$K_J=J_L^T K J_L$$

The estimated joint matrices are given in Table 2. The joint matrices appear to be nearly symmetric. The directions represent the angle between the major axis and horizontal axis in joint space. The directions of the major axes point approximately $-35°$ for all the subjects. When the endpoint stiffness is transformed into the joint stiffness, the minor stiffness becomes even smaller compared to the major stiffness. Note that the stiffness of four subjects have similar major and minor eigenvalues.

The symmetric component of the stiffness matrix $\left(K_{J,symm}=\frac{K_J+K_J^T}{2}\right)$ can be graphically represented as an ellipse characterized by the magnitude (area of ellipse), shape (the ratio of major and minor axes), and the orientation (direction of the major axis). In their arm stiffness study, Mussa-Ivaldi et al.(1985) postulated that the shape and orientation of the stiffness ellipse in joint space is invariant over all subjects tested. This consistency in joint space can also be found in the leg stiffness.

Table 1 Endpoint stiffness matrices

Subject	Joint stiffness matrix (N/m)	Eigensolution Eigenvalue (Direction of Eigenvector)
A	[562.7 587.8 741.2 955.1]	Major: 1448 (56.4°) Minor: 140 (−40°)
B	[269 778.6 294.5 897.2]	Major: 1156 (49°) Minor: 10.4 (−18.4°)
C	[979.1 760.5 797.7 1162.9]	Major: 1855.3 (56.4°) Minor: 286.7 (−42.3°)
D	[536.7 849.4 733.0 1160.2]	Major: 1696.9 (53.8°) Minor: 0.082 (−32.3°)

Table 2 Joint stiffness matrices

Subject	Joint stiffness matrix (Nm/rad)	Eigensolution Eigenvalue (Direction of Eigenvector)
A	[642.1 −511.1 −478.0 387.8]	Major: 1025.4 (−36.9°) Minor: 4.6 (51.3°)
B	[616.8 −366.3 −468.8 279.3]	Major: 895.5 (−37.3°) Minor: 0.6 (59.3°)
C	[778.0 −574.7 −565.8 459.1]	Major: 1208.1 (−37.1°) Minor: 25.0 (52.5°)
D	[849.3 −586.6 −609.0 418.5]	Major: 1267.8 (−35.6°) Minor: 0.0052 (55.5°)

Figure 7 illustrates the stiffness ellipse in joint space. While eigensolutions in Cartesian space vary from subject to subject (Table 1), those in joint space show an impressive consistency, as graphically shown in the figure.

2.3 Simulation of mathematical model

The findings from the experiments raise a question of whether there exists a simple motor program in human leg movement. One of the possible candidates is the equilibrium point hypothesis (Feldman, 1966; Bizzi et al., 1984): command from the central nervous system may generate a series of equilibrium points for a limb, and the "spring-like" properties of the neuromuscular system will tend to drive the motion along a trajectory that follows these intermediate equilibrium postures. Computer simulations of a mathematical model were performed to recreate the experimental results of reaching motion of the human leg in the framework of the equilibrium point control hypothesis.

2.3.1 Mathematical modeling

The two-link planar model of the lower limb, shown in Figure 8, is constrained to move in the sagittal plane, and has two degrees of freedom corresponding to the knee and hip joints. Each segment is modeled as a rigid body, and the segments are connected to each other by frictionless pin joints. The thigh and shank-foot segments have masses m_1 and m_2, respectively. The respective centroidal moments of inertia are I_1 and I_2. Lengths l_1 and l_2 denotes the thigh and shank lengths. Lengths l_{c1} and l_{c2} represent the distance from the proximal joint to the segment mass centers. The approximate distribution of the body mass among the body segments

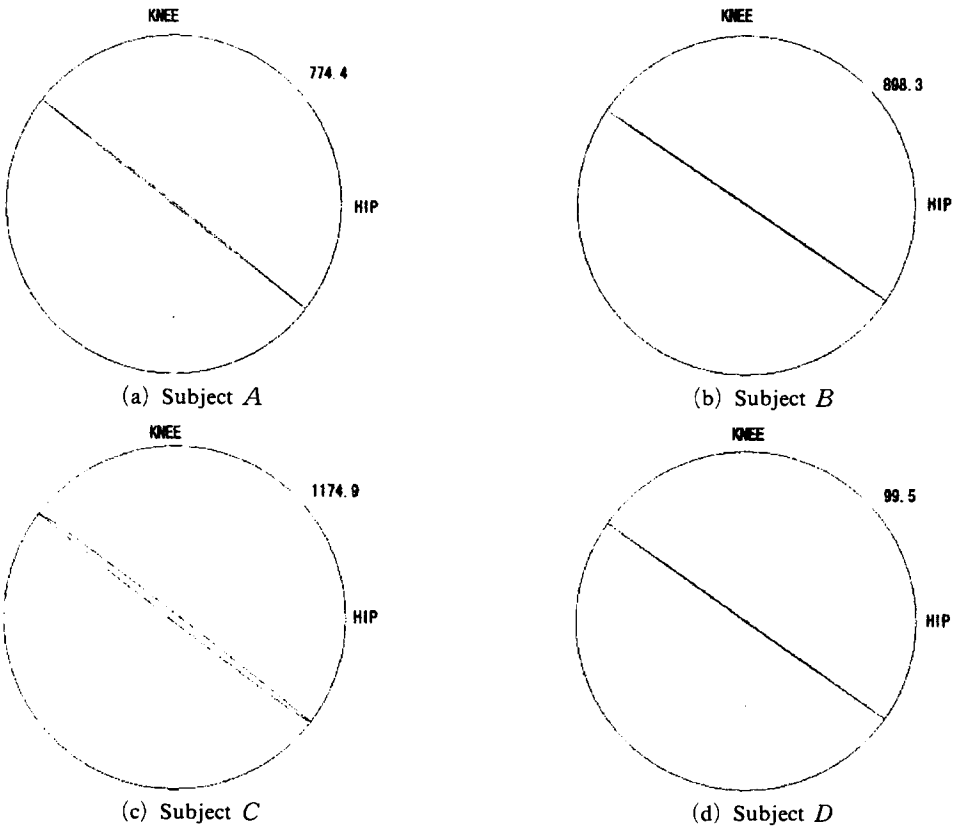

(a) Subject A (b) Subject B

(c) Subject C (d) Subject D

Fig. 7 Stiffness ellipses in joint space

(m_1, m_2, I_1, I_2) was found using a regression model based on the subject's weight and height.

The angular convention Θ (θ_1 and θ_2) describes generalized joint angle, defined with respect to the horizontal line. The angular convention Φ (ϕ_1 and ϕ_2) defines the relative joint flexion between adjacent segments. The absolute angles Θ are more convenient for deriving the dynamic equation, while the relative angles Φ prove more useful in describing virtual trajectories used in the simulation model. The general form for the dynamics equations is given in relative angle coordinates Φ as follows:

$$H(\Phi)\ddot{\Phi}+h(\Phi,\dot{\Phi})+G(\Phi)=Q=Q_{act}+Q_{ext} \tag{1}$$

where

$H(\Phi)=2\times2$ moment of inertia matrix
$h(\Phi,\dot{\Phi})=2\times1$ rate dependent vector
$G(\Phi)=2\times1$ gravitational vector
$Q_{act}=2\times1$ torque vector by muscles forces
$Q_{ext}=2\times1$ torque vector by external forces

Here the gravitational terms are zero since the sagittal plane is in the horizontal plane.

It can also be described in absolute angle coordinates Θ as follows:

$$H^*(\Theta)\ddot{\Theta}+h^*(\Theta,\dot{\Theta})+G^*(\Theta)=T=T_{act}+T_{ext} \tag{2}$$

or

$$H_{11}^*\ddot{\theta}_1+H_{12}^*\ddot{\theta}_2+h_{12}^*\dot{\theta}_2^2+G_1^*=\tau_1=\tau_{act1}+\tau_{ext1}$$

$$H_{21}^*\ddot{\theta}_1+H_{22}^*\ddot{\theta}_2+h_{21}^*\dot{\theta}_1^2+G_2^*=\tau_2=\tau_{act2}+\tau_{ext2}$$

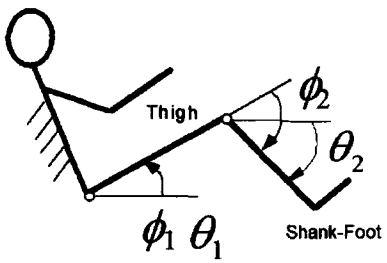

Fig. 8 Two link model of human leg

where the elements of matrices H and h are defined as:

$$H_{11}^*=m_1l_{c1}^2+m_2l_1^2+I_1$$

$$H_{22}^*=m_2l_{c2}^2+I_2$$

$$H_{12}^*=H_{21}^*=-m_2l_1l_{c2}\cos(\theta_1+\theta_2)$$

$$h_{12}^*=h_{21}^*=m_2l_1l_{c2}\sin(\theta_1+\theta_2)$$

The two angle conventions can be related by the following equation.

$$\begin{bmatrix}\phi_1\\ \phi_2\end{bmatrix}=J^*\begin{bmatrix}\theta_1\\ \theta_2\end{bmatrix}$$

where

$$J^*=\begin{bmatrix}1 & 0\\ 1 & 1\end{bmatrix}$$

Torques corresponding to the two sets of coordinate systems can be related as follows:

$$\begin{bmatrix}\tau_1\\ \tau_2\end{bmatrix}=(J^{*-1})^T\begin{bmatrix}Q_1\\ Q_2\end{bmatrix}$$

While muscle force is a complicated function with many variables, the mechanical property of a muscle may be simplified to be a function of muscle length and its rate of change. Hence, leg muscle groups may be modeled as a combination of linear torsional springs and dampers as postulated in the arm models by Hogan (1984) and Flash (1987). Thus, the resultant joint torques are assumed to be dependent only on deviation of the actual trajectory from the equilibrium point trajectory and on joint velocity. The following equation gives the joint control torques as a function of the instantaneous difference of actual and equilibrium point trajectories and joint velocity.

$$Q_{act}=-K_J(\Phi-\Phi_o)-B_J\dot{\Phi} \tag{3}$$

$$\begin{bmatrix}Q_{act1}\\ Q_{act2}\end{bmatrix}=-\begin{bmatrix}k_{HH} & k_{HK}\\ k_{KH} & k_{KK}\end{bmatrix}\begin{bmatrix}\phi_1-\phi_{01}\\ \phi_2-\phi_{02}\end{bmatrix}-\begin{bmatrix}b_{HH} & b_{HK}\\ b_{KH} & b_{KK}\end{bmatrix}\begin{bmatrix}\dot{\phi}_1\\ \dot{\phi}_2\end{bmatrix}$$

$$K_J=\begin{bmatrix}k_{HH} & k_{HK}\\ k_{KH} & k_{KK}\end{bmatrix}$$

$$B_J=\begin{bmatrix}b_{HH} & b_{HK}\\ b_{KH} & b_{KK}\end{bmatrix}$$

where

Q_{act}=torque vector of muscle forces
Θ, $\dot{\Theta}$= vector of joint angles and rates
Θ_o=vector of equilibrium point joint angles
K_J=joint stiffness matrix
B_J=joint damping matrix

Here, subscripts H and K denote hip and knee joints, respectively.

Additional assumptions for the EPC (Equilibrium Point Control) model in foot reaching motion are as follows:

(1) Linear and time-invariant impedance:

Stiffness matrix $\boldsymbol{K}_J$ and damping matrix $\boldsymbol{B}_J$ are assumed to be linear about the equilibrium position and the velocity, respectively. They are also constant over the entire range of movements regardless of the posture.

(2) Minimum-jerk equilibrium point trajectory as a motor program:

The driving input to the EPC model is an equilibrium point trajectory that is a straight line in Cartesian space from the initial position x_i to the final position x_f. This trajectory has a minimum-jerk velocity profile taking the equilibrium point from the start to the finish:

$$x(t)=x_i+(x_f-x_i)(10\tau^3-15\tau^4+6\tau^5) \quad (4)$$

$$v(t)=(x_f-x_i)(30\tau^2-60\tau^3+30\tau^4)/t_f \quad (5)$$

where $\tau=t/t_f$.

Here, τ is normalized time, and t_f is the duration of movement.

Motor programs for all reaching movements of the EPC model can be generated simply by translating and scaling the minimum-jerk functions described above.

2.3.2 Simulation of foot reaching movement

The procedure to simulate reaching motion of the foot is similar to works of Flash (1987) for arm movement. With a minimum-jerk equilibrium point trajectory and the measured postural stiffness as simulation inputs, a point-to-point reaching motion was recreated and compared with the experimentally measured movement. Figure 9 illustrates the simulation procedure. The equilibrium point trajectory in Cartesian coordinates is transformed into leg joint coordinates Φ using the geometry of the two-link leg model. Under the assumption that stiffness is greater in motion than in static posture, the value of each element in the measured stiffness matrix was multiplied by a scaling factor. The scaling factor ranged between 9 and 13 for outward reaching motion. For inward motion, the scaling factor was around 5. Also, the damping matrix is assumed to be proportional to the scaled stiffness matrix with a time constant $\tau=\boldsymbol{B}_J/\boldsymbol{K}_J$. The time constant was chosen to be 0.05 sec as in works of Flash (1987) and Won (1993) for arm movement. It was inferred that the mechanical properties of muscles in the leg and the arm are nearly identical.

Simulation results from four subjects are shown in Figures 10 and 11. Figure 10 compares the simulated trajectories with the actual trajectories from measurement. All the motions were outward with the exception of subject A. While the simulated paths closely resemble the measured

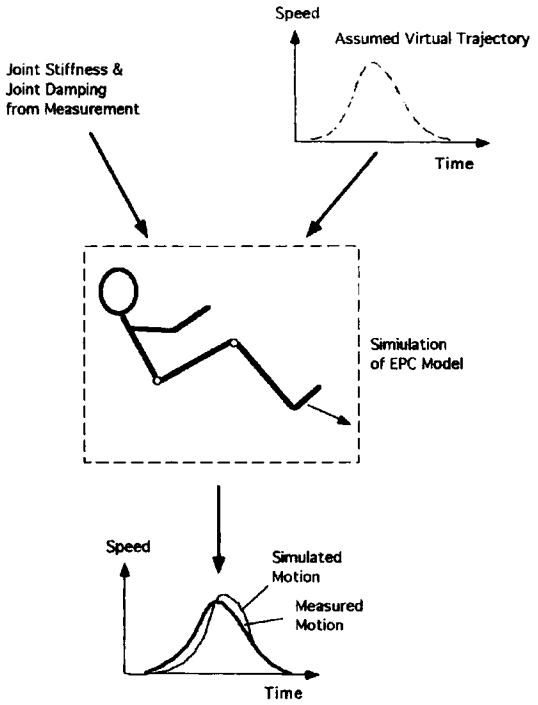

Fig. 9 Simulation procedure

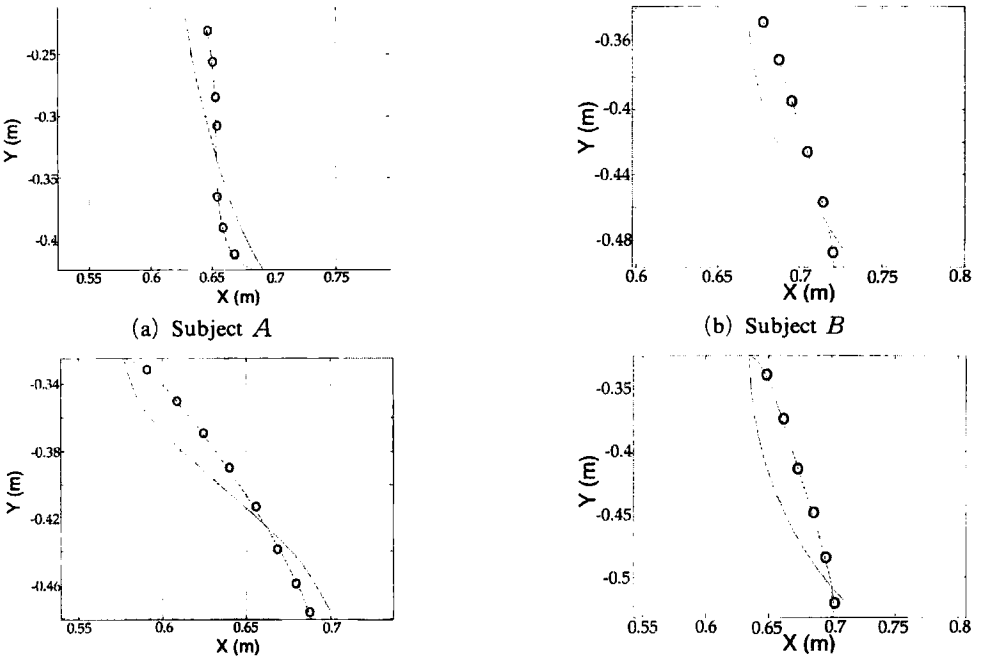

(a) Subject A (b) Subject B

(c) Subject C (d) Subject D

Fig. 10 Comparison of Trajectories from measurement and simulation
(Solid line : Measured Trajectory, Dotted line : Simulated trajectory)

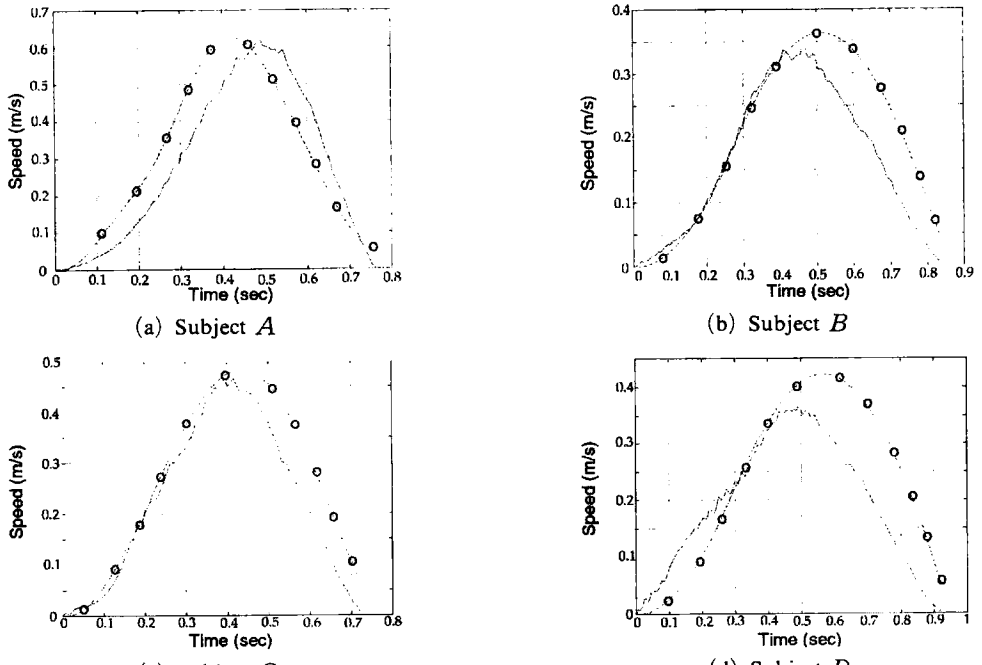

(a) Subject A (b) Subject B

(c) Subject C (d) Subject D

Fig. 11 Comparison of Velocity profiles from measurement and simulation
(Solid line : Measured Trajectory, Dotted line : Simulated trajectory)

ones, the paths resulting from the simulations failed to reproduce the unique curvature existent in those from measurement. Figure 11 compares simulated and measured velocity profiles. While the simulations produced the typical bell-shaped velocity profiles, the profile peaks did not coincide with those of measured velocities.

Simulated trajectories showed kinematic features such as straight paths and bell-shaped velocity profiles. With a single minimum-jerk equilibrium trajectory as an input, the features of simulated trajectories paralleled those of measured movement. As postulated by Flash (1987) and Won (1993) in their arm motion studies, simple foot reaching motions may be controlled by a single equilibrium point trajectory.

2.3.3 Leg stiffness estimation

This section attempts to estimate stiffness from the difference between measured reaching motion and assumed equilibrium point trajectory. First, inverse dynamics of the two-link leg model calculated joint torques at hip and knee joints from the measured movement. Using these calculated joint torques along with the measured movement and assumed minimum-jerk equilibrium point trajectory, stiffness was estimated and compared with the measured stiffness. This procedure is nearly identical to the simulation of the three-link model by Jackson (1997). Figure 12 illustrates the estimation procedure.

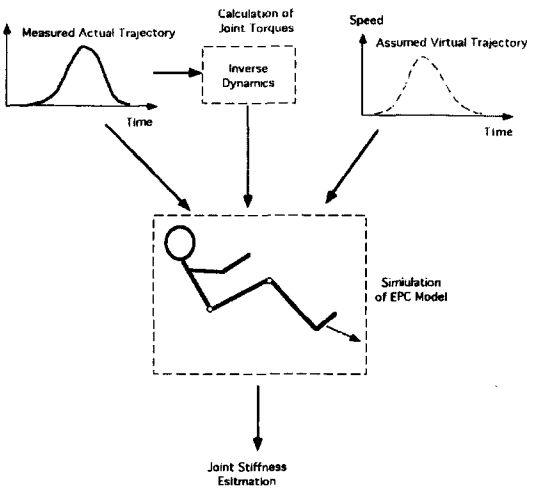

Fig. 12 Estimation procedure

The stiffness and damping matrices are constrained to be symmetric ($K_{HK}=K_{KH}$, $B_{HK}=B_{KH}$), which seems reasonable from the results of stiffness measurements. Based on the symmetry of the matrices, three independent stiffness elements and three independent damping elements were estimated. The joint torques at hip and knee joints were estimated using the inverse dynamics solution. Since joint torques, joint angles and their rates are determined, Equation 3 provides two simultaneous equations with six unknowns at each sampling time. These equations can be restated in a form conducive to a least squares estimate of the unknown elements :

$$\begin{bmatrix} \cdot & & & & & \\ \cdot & & & & & \\ \cdot & & & & & \\ \Delta\phi_{Hi} & 0 & \Delta\phi & \dot{\phi}_{Hi} & 0 & \dot{\phi}_{Ki} \\ 0 & \Delta\phi_{Ki} & \Delta\phi & 0 & \dot{\phi}_{Ki} & \dot{\phi}_{Hi} \\ \cdot & & & & & \\ \cdot & & & & & \\ \cdot & & & & & \end{bmatrix} \begin{bmatrix} k_{HH} \\ k_{KK} \\ k_{HK} \\ b_{HH} \\ b_{KK} \\ b_{HK} \end{bmatrix} = \begin{bmatrix} \cdot \\ \cdot \\ \cdot \\ -Q_{Hi} \\ -Q_{Hi} \\ \cdot \\ \cdot \\ \cdot \end{bmatrix} \quad (6)$$

where

$\Delta\phi=\phi-\phi_o$
ϕ_o=equilibrium joint angle for joint
i=sample number

This can be presented in a matrix form as follows :

$$A\cdot X=T$$

where

A=matrix of joint angle deviation and joint rates
X=vector of stiffness and damping elements
T=vector of joint torques

Using least-squares estimation, the stiffness and damping elements can be estimated by :

$$X=(A^T\cdot A)^{-1}A^T T \quad (7)$$

where

X=estimated stiffness and damping vector

Each sample provides two independent equations, which means at least three data samples are required to estimate the six independent elements.

The estimated stiffness matrices from four subjects are given in Table 3. The estimations are compared with the stiffness from measurement in the table. The most puzzling result from this estimation is the large dispersion in estimates of stiffness magnitudes. While the signs of the matrix elements show consistency, the magnitudes ranged widely from the order of 100 to 1000. In Figure 13, the shape of the estimated stiffness matrix appears to be similar to that of the measured matrix in spite of the dispersion in magnitudes. Despite some discrepancy the equilibrium point control model recreates qualitative features of experimental results of planar leg motion.

Table 3 Joint stiffness estimates

Subject	Stiffness matrix from estimation (N/m/rad)	Stiffness matrix from measurement (Nm/rad)
A	$\begin{bmatrix} 247.0 & -121.5 \\ -121.5 & 245.4 \end{bmatrix}$	$\begin{bmatrix} 642.1 & -511.1 \\ -478.0 & 387.8 \end{bmatrix}$
B	$\begin{bmatrix} 697.1 & -144.7 \\ -144.7 & 27.5 \end{bmatrix}$	$\begin{bmatrix} 616.8 & -366.3 \\ -468.8 & 279.3 \end{bmatrix}$
C	$\begin{bmatrix} 3663.2 & -1263.7 \\ -1263.7 & 568.9 \end{bmatrix}$	$\begin{bmatrix} 778.0 & -574.7 \\ -565.8 & 459.1 \end{bmatrix}$
D	$\begin{bmatrix} 1335.4 & -674.4 \\ -674.4 & 343.5 \end{bmatrix}$	$\begin{bmatrix} 849.3 & -583.6 \\ -609.0 & 418.5 \end{bmatrix}$

This discrepancy between estimated and measured stiffness seems to result from the sensitivity of the stiffness estimate to the difference of the assumed equilibrium point trajectory and measured trajectory. If the equilibrium point trajectory is too far from or too close to the measured trajectory, the stiffness estimate will be in error and will be too small or too large in magnitude, respectively. Moreover, selecting the starting and finishing points of the reaching motion from measured data was not trivial. Unfortunately these values have a strong effect on shaping the equilibrium point trajectory and in

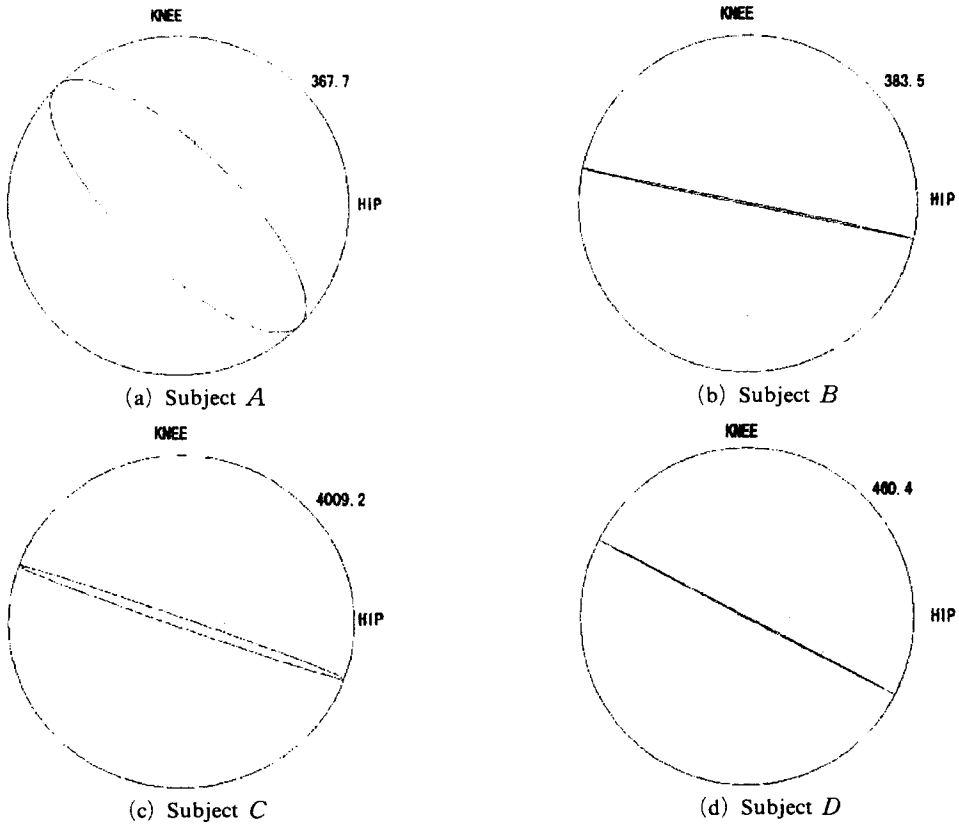

(a) Subject *A* (b) Subject *B*

(c) Subject *C* (d) Subject *D*

Fig. 13 Comparison of stiffness ellipses

turn, on the stiffness estimation. Also, the inertia parameters used in the simulations were calculated from simple regression equations based only on gender, height, and weight of the subject. It is unclear whether these parameters are sufficiently accurate for the purpose of the estimation. Since human legs have relatively large inertia, errors in the inertia parameter may have had a considerable effect on the stiffness estimation results.

3. Discussion

The point-to-point movement by the foot showed nearly identical features to those of planar hand reaching motion demonstrated in previous arm experiments (Morasso, 1981; Abend et al., 1982; Flash, 1987; Won, 1993). While all the trajectories of foot reaching movements were fairly straight, movements with a locked ankle showed unique curvature. The velocity profile during point-to-point motion had a characteristic bell shape. Arm movement experiments showed that the hand of the subject generates essentially a straight path from start to finish with a characteristic bell-shaped tangential velocity profile during self-placed point-to-point reaching movements (Morasso, 1981; Abend et al., 1982). In measuring stiffness, the experimenter relied on the subjects to not resist voluntarily against the applied displacement. However, it is inevitable that the subjects respond to the disturbance by applying sudden force to the manipulator. The validity of the data was checked by examining its consistency over a number of different trials and subjects. Mussa-Ivaldu et al.(1984) showed that consistent results could be achieved with this "do-not-resist-voluntarily" instruction.

The features found in experiments were similar to those which can be found in arm motion studies (Mussa-Ivaldi, 1985; Flash, 1987). In her arm movement simulations, Flash (1987) showed that the equilibrium point control hypothesis is competent to predict simple point-to-point reaching motion. As one of the candidates for the motor program producing foot reaching motion, this equilibrium point control hypothesis was tested by numerical simulations. The equilibrium point control model seems to consistently recreate experimental results.

Characterization of human limb impedance is applicable to the design and configuration of a wide variety of human-machine interface and human-object interaction tasks. For instance, findings in this research may provide some new insight on human-brake system design. Analyzing a simple reaching motion of the leg may help understand the mechanisms underlying the driver's maneuver of the brake pedal. Based on human leg motion analysis, the braking motion is modeled as:

(1) A two degrees-of-freedom motion with free hip and knee joints

(2) A simple open-loop reaching motion in free space followed by impeded motion in force field (brake pedal).

The fact of preprogrammed braking motion suggests that drivers have the same command from the central nervous system (CNS) in movements both in free space and in contact with the brake pedal. It also suggests that the input commands are the same for different brake pedal impedances. It can be inferred that further pedal depression will be induced with a softer brake pedal under the same CNS command. In brake system design these features should be taken into consideration (Park, 1999).

Analyzing a certain aspect of the leg motion helped illuminate the mechanisms underlying drivers' maneuver of the brake pedal. In this study, a rather simple procedure was used in investigating leg motion. In examining the motor control of human limbs, however, precise measurement and rigorous analysis are critical and needed. The two-dimensional motion measurement may be replaced by three-dimensional multi-joint motion capture techniques (Bregler, 1997; Cipolla and Pentland, 1998; Mun, 2003). This may result in a more accurate analysis of human motion.

4. Conclusions

As a precursor study for brake system design, the following features of human leg movement were characterized through experiments :

(1) Foot reaching motion with locked ankle travels in a slightly curved path.

(2) Foot reaching motion with locked ankle has a bell-shaped speed profile.

(3) Foot motion is much slower than hand motion.

(4) Foot reaching motion can be modeled as a preprogrammed open-loop motion.

The findings in the experiments suggest a simple open-loop motor control scheme in leg motion. As a possible candidate, an equilibrium point control model was consistent in recreating the experimental data in numerical simulations. Analyzing a simple reaching motion of the leg helped illuminate the mechanisms underlying the driver's maneuver of the brake pedal. Findings in this research may provide some new insight on human-brake system design. A foreseeable extension of this research would be to design brake systems that take advantage of the open-loop nature of human motor control.

Acknowledgment

The author would like to thank all the experimental subjects for their participation in our study.

References

Abend, W., Bizzi, E. and Morasso, P., 1982, *Human Arm Trajectory Formation*, Brain, Vol. 105, pp. 331~348.

Albus, J., 1975, A New Approach to Manipulator Control : The Cerebellar Model Articulation Controller (CMAC), J. Dynamics. Sys., *Meas. & Control*, Vol. 97, pp. 220~227.

Arbib, M., 1972, The Metaphorical Brain : An Introduction to Artificial Intelligence and Brain Theory, Interscience, New York.

Bernstein, N., 1967, The Coordination and Regulation of Movements, Pergamon Press, New York.

Bizzi, E., Accomero, N., Chapple, W. and Hogan, N., 1984, Posture Control and Trajectory Formation During Arm Movement, J. Neurosci., Vol. 4, pp. 2738~2744.

Bizzi, E., Hogan, N., Mussa-Ivaldi, F. and Giszter, S., 1992, "Does the Nervous System Use Equilibrium-Point Control to Guide Single and Multiple Joint Movements?," *Behavioral and Brain Sciences*, Vol. 15, pp. 603~613.

Colgate, J. and Hogan, N., 1988, Robust Control of Dynamically Interacting Systems, *Int. J. Control*, Vol. 48, pp. 65~88.

Feldman, A., 1966, Functional Tuning of the Nervous System with Control of Movement or Maintenance of a Steady Posture, II : Controllable Parameters of the Muscle, Biophysics, Vol. 11, pp. 565~578.

Flash, T., 1987, The Control of Hand Equilibrium Trajectories in Multi-Joint Arm Movements, Biol. Cybern., Vol. 57, pp. 257~274.

Gomi, H. and Kawato, M., 1996, Equilibrium-Point Control Hypothesis Examined by Measured Arm Stiffness during Multijoint Movement, Science, Vol. 272, pp. 117~120.

Hogan, N., 1989, Controlling Impedance at the Man/Machine Interface, Proceedings of the 1989 IEEE international conference on robotics and automation.

Hollerbach, J. and Atkeson, C., 1987, Deducing Planning Variables from Experimental Arm Trajectories : Pitfalls and Possibilities, *Biological Cybernetics*, Vol. 56, pp. 279~292.

Jackson, D., 1997, Development of Full-Body Models for Human Jump Landing Dynamics and Control, Ph. D. Thesis, Department of Aeronautics and Astronautics, Massachusetts Institute of Technology, Cambridge, MA.

Morasso, P., 1981, Spatial Control of Arm Movements, Exp. Brain Res., Vol. 42, pp. 223~227.

Mun, J., 2003, A Method for the Reduction of Skin Marker Artifacts During Walking Application to the Knee, *KSME International Journal*, Vol. 17, No. 6, pp. 825-835.

Mussa-Ivaldi, F., Hogan, N. and Bizzi, E., 1985, Neural, Mechanical, and Geometric Factors Subserving Arm Posture in Humans, *J. of Neuroscience*, Vol. 5, No. 10, pp. 2732~2743.

Paines, J., 1987, Optimization of Manual Control Dynamics for Space Telemanipulation : Impedance Control of a Force Reflection Hand Controller, S. M. Thesis, Department of Aeronautics and Astronautics, Massachusetts Institute of Technology, Cambridge, MA.

Park, S., 1999, Driver-Vehicle Interaction in Braking, Ph. D. Thesis, Department of Mechanical Engineering, Massachusetts Institute of Technology, Cambridge, MA.

Pennisi, E., 1996, Tilting against a Major Theory of Movement Control, Science, Vol. 272, pp. 32~33.

Saltzman, 1979, E., Levels of Sensorimotor Representation, *J. Math. Psych.*, Vol. 20, pp. 91~163.

Raibert, M., 1976, A State Space Model for Sensorimotor Control and Learning. MIT Artif. Intel. Memo, No. 351.

Shadmehr, R. and Mussa-Ivaldi, F., 1994, Adaptive Representation of Dynamics during Learning of a Motor Task. *Journal of Biomechanics*, Vol. 29, pp. 1137~1146.

Won, J., 1993, The Control of Constrained and Partially Constrained Arm Movement, S. M. Thesis, Department of Mechanical Engineering, Massachusetts Institute of Technology, Cambridge, MA.

Woodson, W. and Conover, D., 1964, Human Engineering Guide for Equipment Designers, University of California Press.